

Mechanism underlying the anti-diabetic potential of bee venom as compared to bone marrow mesenchymal stem cells in the diabetic rat tongue

Israa Ahmed Radwan^{1,A,C,D,F}, Dina Rady^{1,A,B,D–F}, Mohamed Ramadan^{2,A,E,F}, Sara El Moshly^{1,A,B,D,F}

¹ Department of Oral Biology, Faculty of Dentistry, Cairo University, Egypt

² Specialized Dental Hospital, Armed Forces Medical Complex, Kobry El Qobba, Cairo, Egypt

A – research concept and design; B – collection and/or assembly of data; C – data analysis and interpretation;

D – writing the article; E – critical revision of the article; F – final approval of the article

Dental and Medical Problems, ISSN 1644-387X (print), ISSN 2300-9020 (online)

Dent Med Probl. 2024;61(1):53–64

Address for correspondence

Dina Rady

E-mail: dina.radi@dentistry.cu.edu.eg

Funding sources

None declared

Conflict of interest

None declared

Acknowledgements

None declared

Received on June 3, 2022

Reviewed on July 27, 2022

Accepted on August 23, 2022

Published online on February 29, 2024

Abstract

Background. Diabetes mellitus (DM) is a critical chronic metabolic disease. Several treatment modalities are currently under investigation. Both bee venom (BV) and bone marrow mesenchymal stem cells (BMSCs) can possibly offer an approach for treating type I diabetes.

Objectives. The aim of the present study was to investigate the mechanism underlying the anti-diabetic effect of BV as compared to BMSCs on the tongue mucosa of diabetic rats.

Material and methods. A total of 52 male albino rats were used in the current study. The rats were randomly assigned into 4 groups: group 1 (control); group 2 (streptozocin (STZ)); group 3 (BV-treated); and group 4 (BMSC-treated). Diabetes mellitus was induced via an intraperitoneal (IP) injection of STZ in the rats from groups 2, 3 and 4. Following the diagnosis of DM, the rats in group 3 were injected with a daily dose of 0.5 mg/kg of BV, while the rats in group 4 were treated with a single injection of BMSCs. All rats were euthanized after 4 weeks, and their tongues were dissected and divided into halves. The right halves of the tongues were utilized for the histological examination, followed by morphometric analysis. In contrast, the left halves were used to detect the local gene expression of transforming growth factor beta 1 (TGF- β 1) and vascular endothelial growth factor (VEGF).

Results. Group 2 revealed marked disruption in the morphology of the fungiform and filiform papillae, and atrophic epithelial changes in both dorsal and ventral surface epithelium as compared to other groups. Group 4 showed a significantly larger number of taste buds, and a higher gene expression of TGF- β 1 and VEGF as compared to groups 2 and 3. Additionally, BV and BMSCs effectively increased the thickness of dorsal and ventral surface epithelium as compared to group 2.

Conclusions. Treatment with BMSCs was associated with significant improvement in the morphology and number of lingual epithelial cells and taste buds in the tongues of diabetic rats as compared to BV-treated rats, which was due to the local upregulation of TGF- β 1 and VEGF gene expression.

Keywords: bee venom, diabetes, streptozocin, bone marrow mesenchymal stem cells

Cite as

Radwan IA, Rady D, Ramadan M, El Moshly S. Mechanism underlying the anti-diabetic potential of bee venom as compared to bone marrow mesenchymal stem cells in the diabetic rat tongue. *Dent Med Probl.* 2024;61(1):53–64. doi:10.17219/dmp/152924

DOI

10.17219/dmp/152924

Copyright

Copyright by Author(s)

This is an article distributed under the terms of the

Creative Commons Attribution 3.0 Unported License (CC BY 3.0)

(<https://creativecommons.org/licenses/by/3.0/>).

Introduction

Diabetes mellitus (DM) is considered a critical chronic metabolic disease due to a prompt rise in the number of diagnosed patients, especially over the last 2 decades.¹ Diabetes mellitus is characterized by high blood glucose levels, which, if not controlled efficiently, leads to end-organ damage within the genitourinary, cardiovascular and neurological systems.² These characteristics make DM a condition that needs proficient and long-standing medical care in order to control elevated blood glucose levels and prevent complications.³ Several drugs used to treat DM have adverse effects, which necessitates a search for other modalities that could overcome these side effects, without imposing a financial strain on the patient.⁴

Bee venom (BV) is composed of different types of proteins, enzymes and non-peptide components. The proteins include melittin, apamin, adolapin, and mast cell degranulating (MCD) peptide. The enzymes found in BV include α -glucosidase, phosphatase, phospholipase B, phospholipase A2, and hyaluronidase. Additionally, non-peptide components, such as histamine, dopamine and norepinephrine, have been identified in BV.⁵ Due to its therapeutic effects, BV has been used as a drug in the treatment of many diseases, such as cardiovascular, neurological, hematological, musculoskeletal, and dermatological diseases.^{6,7}

The anti-diabetic effect of BV can be associated with melittin and phospholipase A2, a polypeptide and an enzyme that increase the secretion of insulin from pancreatic β -cells via the depolarization of the β -cell membrane.⁸ Taking into account the abovementioned properties, BV could be considered a therapeutic agent in the treatment of DM.

Bone marrow mesenchymal stem cells (BMSCs) are multipotent, self-renewing cell populations that exhibit a marked therapeutic potential because of their ability to differentiate into the 3 germ layer lineages. Furthermore, they can migrate toward the damaged sites when administered systemically. In damaged tissues, they can improve recovery, as they differentiate into cells specific to the tissue, and produce paracrine mediators and trophic factors that possess anti-apoptotic properties and stimulate cell proliferation.^{9–11}

The BMSC therapy offers a cell-based approach for treating type I diabetes. These cells can differentiate into insulin-producing cells, and also show immunosuppressive activity, exerting ameliorative effects on injured tissues.^{12,13}

Diabetes mellitus is often related to prolonged or insufficient healing; this is attributed to the abnormal inflammatory response and a reduction in the production of growth factors, leading to impaired neovascularization and compressed collagen matrices.¹⁴

Transforming growth factor beta 1 (TGF- β 1) is known to regulate the chemotaxis of immune and inflammatory

cells, cellular differentiation, and induce the accumulation of extracellular matrix proteins.¹⁵ Indeed, defective TGF- β 1 signaling contributes to delayed wound healing in diabetes.¹⁶ Vascular endothelial growth factor (VEGF) promotes tissue repair via increasing vascular permeability, as well as the proliferation and migration of the pre-existing endothelial cells.¹⁷

The present study aimed to evaluate and compare the potential anti-diabetic effects of BV and BMSCs against the histological and molecular changes in the tongue in streptozotocin (STZ)-induced diabetic albino rats.

Material and methods

Bee venom

The BV samples were collected from the colonies of Italian and Carniolan hybrid honeybees (*Apis mellifera*), using a BV collector (an electric shock device, VC-Starter kit; IGK electronics Ltd., Varna, Bulgaria) at the National Research Center, Cairo, Egypt. The dried BV material was transferred to a proper container and was solubilized in distilled water to reach a concentration of about 0.1 mg/mL.¹⁸

Bone marrow mesenchymal stem cells (BMSCs)

Bone marrow mesenchymal stem cells were isolated from the femora and tibiae of 6 Wistar donor rats (6-week-old, male, weighing 100 \pm 20 g). The isolation and propagation of BMSCs was conducted under aseptic conditions, 14 days before the experimental procedures, as previously described.¹⁹

The femora and tibiae were flushed with Dulbecco's Modified Eagle Medium (DMEM) (Gibco-BRL, Gaithersburg, USA) supplemented with 10% fetal bovine serum (FBS) (Gibco-BRL), using an 18-gauge needle. The cells were cultured in a culture medium supplemented with 1% penicillin–streptomycin (Gibco-BRL) in an incubator, at 37°C in a humidified atmosphere (5% CO₂). Upon reaching 80–90% confluence, the cultures were washed twice with phosphate-buffered saline (PBS) and the cells were trypsinized with 0.25% trypsin in 1 mM ethylenediaminetetraacetic acid (EDTA) (Gibco-BRL) at 37°C for 5 min. Then, the cells were centrifuged at 2,400 rpm for 20 min, re-suspended with a serum-supplemented medium and incubated in a Falcon® culture flask with a surface area of 50 cm². On day 14, the adherent colonies of cells were trypsinized and counted.¹⁹

Culture confluence was monitored using an inverted light microscope (Olympus, Center Valley, PA, USA) with a digital camera (Nikon, Tokyo, Japan).

Characterization of BMSCs

Flow cytometry was performed to identify BMSCs. After blocking in 0.5% bovine serum albumin (BSA) and 2% FBS in PBS, 100,000 cells were incubated in the dark at 4°C for 20 min with the following monoclonal antibodies: FITC CD 90 (PN IM1839U; Beckman Coulter, Brea, USA); and PE CD 34 (PN IM1871U; Beckman Coulter). Mouse-isotype PE antibodies (Beckman Coulter) were used as controls (the dilution of all antibodies at 1:1,500). The cells were washed and suspended in 500 µL of the fluorescence-activated cell sorting (FACS) buffer, and analyzed using the Cytomics FC 500 flow cytometer with the CPX software, v. 2.2 (Beckman Coulter).

Animals

This study was approved by the Institutional Animal Care and Use Committee (IACUC) at Cairo University, Egypt (approval No. CU III F 74 18). This research was conducted in compliance with the ARRIVE (Animal Research: Reporting of In Vivo Experiments) guidelines and regulations (<https://arriveguidelines.org>).

A sample size of 52 (13 per group) was estimated to be sufficient, assuming an effect size of 0.6, a power of 0.8, a two-sided hypothesis test, and a significance level of 0.05 for categorical and numerical data. Fifty-two healthy adult male albino rats, weighing about 150–200 g, with normal glucose levels, were used. All animals were housed in a sterile, controlled environment (room temperature of 25 ±5°C under a natural light, 12-hour dark/light cycle). They were fed with standard, ordinary, commercial rat pellets and were provided water ad libitum. The maintenance and care of the experimental animals conformed with the International Guiding Principles for Biomedical Research Involving Animals. The animals were randomly divided into 4 groups of 13 animals, using the Random Sequence Generator program (<https://www.random.org>).

Induction of experimental diabetes

Streptozotocin (Sigma-Aldrich, St. Louis, USA)²⁰ was used for inducing type I diabetes by a single intraperitoneal (IP) injection of STZ (60 mg/kg b.w.) into fasted rats. The rats were considered diabetic when their random blood glucose reading was >300 mg/dL at 72 h of the STZ

injection.²¹ Diabetes was allowed to stabilize in the STZ-injected rats for 1 week. The assessment of blood glucose levels was performed weekly in all diabetic rats until the end of the experiment. In all groups, the blood samples were obtained from the tail vein and the blood glucose level was expressed in mg/dL.

Animal grouping

The animals were randomly divided into 4 groups, 13 animals in each, occupying separate cages (Table 1). Group 1 (control) comprised normal healthy rats, which were given a physiological saline solution (0.9% NaCl). The veterinarian administered the STZ induction. Then, the STZ-treated rats were randomly divided into 3 groups (2–4). The rats from group 2 (the STZ group) received a single IP injection of STZ (60 mg/kg in freshly prepared 0.1 mol/L citrate buffer (pH 4.5)) and were left untreated. The diabetic rats from group 3 (the BV-treated diabetic group) were injected IP with a daily dose of 0.5 mg/kg of BV for 4 weeks.²² The diabetic rats from group 4 (BMSC-treated diabetic group) were administered a single intravenous (IV) injection of the previously cultured BMSCs at a dose of 1 million cells/mL in PBS.²³

Animal sacrifice and tissue preparation

All rats were euthanized by an intracardiac overdose of sodium thiopental (80 mg/kg) after 4 weeks. The tongues were dissected into 3 parts: two halves of the anterior two-thirds; and the posterior one-third of the tongue.

The specimens from the right halves of the anterior two-thirds and the posterior one-third of the tongue were prepared for the histopathological examination. Serial sections of 5 µm of the tongue tissues were cut and subjected to the following:

- the fluorescence detection of the PKH26-labeled BMSCs in the unstained paraffin sections with the use of a fluorescence microscope; and
- the hematoxylin and eosin (H&E) staining for histological evaluation.

The specimens from the left halves of the anterior two-thirds were used to measure the expression of both TGF-β1 and VEGF.

The assessment steps were carried out blindly by the investigators.

Table 1. Experimental design of the study

Group	n	Induction of diabetes	Treatment
Group 1 (control)	13 rats	none	saline solution
Group 2 (STZ)	13 rats	IP injection of STZ	none
Group 3 (STZ + BV)	13 rats	IP injection of STZ	injected IP with a daily dose of 0.5 mg/kg of BV for 4 weeks
Group 4 (STZ + BMSCs)	13 rats	IP injection of STZ	a single IV injection of the previously cultured BMSCs at a dose of 1 million cells/mL in PBS

STZ – streptozotocin; BV – bee venom; BMSCs – bone marrow mesenchymal stem cells; IP – intraperitoneal; IV – intravenous; PBS – phosphate-buffered saline.

Morphometric analysis

The specimens were examined using light microscopy (Leica, St. Gallen, Switzerland) under $\times 400$ magnification. The data was obtained using the Leica Qwin 500 image analyzer computer system (Leica Biosystems, Cambridge, UK). Image analysis was done using the ImageJ software, v. 1.53d (<https://imagej.net/ij>).²⁴ The image analysis system was used to assess the dorsal and ventral epithelial thickness, the thickness of each cell layer,²⁵ and the area of the connective tissue papillae.²⁶ For each criterion, 5 non-overlapping microscopic fields were randomly selected and evaluated. As previously described, the number of taste buds per circumvallate papilla was assessed.²⁷

Quantitative real-time polymerase chain reaction

To analyze the mRNA levels of TGF- $\beta 1$ and VEGF, the total RNA-containing genes were determined by the quantitative real-time polymerase chain reaction (qRT-PCR). RNA was isolated with the QIAzol lysis reagent (Qiagen, Venlo, the Netherlands). Complementary DNA (cDNA) was produced using a cDNA synthesis kit (Applied Biosystems, Waltham, USA), and qRT-PCR was performed using the StepOnePlus™ RT-PCR system (Applied Biosystems), following the standardized protocols. The expression of genes was normalized relative to the mean critical threshold (CT) values with the $\Delta\Delta CT$ method, using glyceraldehyde 3-phosphate dehydrogenase (GAPDH) mRNA as an internal control. The primers for TGF- $\beta 1$, VEGF and GAPDH are listed in Table 2.

Statistical analysis

The values are presented as mean and standard deviation ($M \pm SD$). The Kolmogorov–Smirnov test indicated that the data was normally distributed. The one-way analysis of variance (ANOVA) was used to assess differences between the groups, and Tukey's post hoc test was applied when ANOVA yielded a significant difference. The significance level was set at $p < 0.05$. Statistical analysis was performed using the Minitab® software, v. 18.1 (<https://www.minitab.com/en-us/support/downloads>).

Table 2. Primer sequences specific for each gene

Gene	Primer sequence from 5' to 3'
TGF- $\beta 1$	forward: TAC CAT GCC AAC TTC TGT CTG GG A reverse: ATG TTG GAC AAC TGC TCC ACC TTG
VEGF	forward: CAC CAC CAC ACC ACC ATC reverse: GCG AAT CCA GTT CCA CGAG
GAPDH	forward: ACA GTC CAT GCC ATC ACT GCC reverse: GCC TGC TTC ACC ACC TTC TTG

Results

Characteristics of BMSCs in the culture

The cultured BMSCs revealed a fibroblast-like morphology and they adhered to the tissue culture substrate within 24–48 h. They reached confluence within 7–14 days (Fig. 1).

Fluorescence detection

The examination of the unstained paraffin sections with the use of a fluorescence microscope was performed to detect and track the PKH26-labeled BMSCs. The tongue specimens from group 4 injected with the PKH26-labeled BMSCs showed red fluorescent cells within the tongue tissue (Fig. 2).

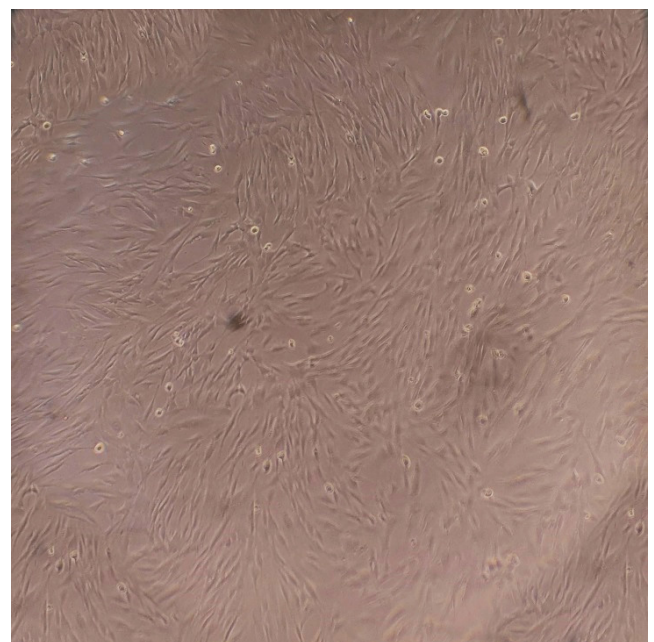


Fig. 1. Microscopic observation shows that the isolated bone marrow mesenchymal stem cells (BMSCs) have a fibroblast-like and spindle-shaped morphology ($\times 100$)

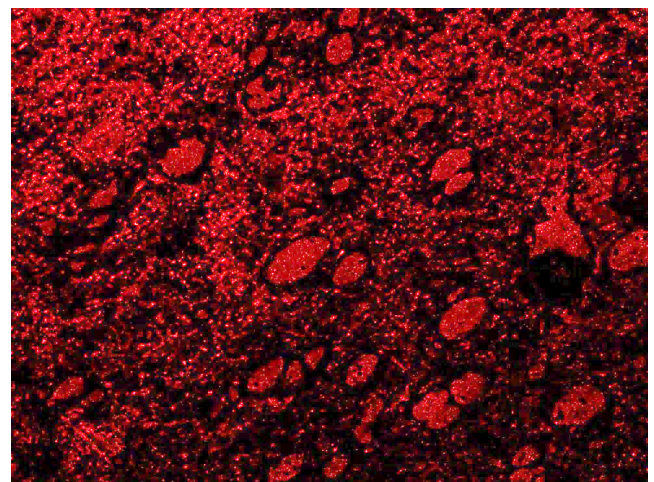


Fig. 2. Photomicrograph of group 4 tongue specimens, showing the PKH26-labeled bone marrow mesenchymal stem cells (BMSCs), which appear as red fluorescent cells

Characterization of BMSCs

The cells were characterized by flow cytometry through the use of surface markers. The results showed that most of the BMSCs were positive for CD90 and negative for CD34 (Fig. 3).

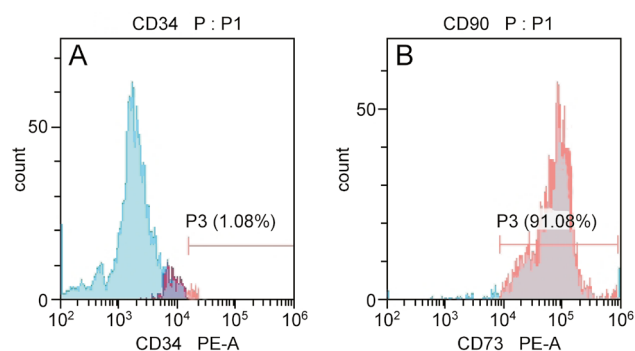


Fig. 3. Flow cytometric analysis showing the expression level of CD90⁺ (A) and CD34[−] (B) in the bone marrow mesenchymal stem cells (BMSCs) isolated from the rats

Biochemical analysis

At 3 weeks, BMSCs significantly reduced blood glucose levels as compared to the STZ group. At 4 weeks, both BV and BMSC treatment were associated with a significant reduction in blood glucose levels as compared to the STZ group (Table 3).

Histopathological examination

Upon the examination of group 1 (the control group), the fungiform papillae displayed a normal mushroom-like appearance with barrel-shaped taste buds and well-defined connective tissue (Fig. 4A). Normal thread-like filiform papillae with orthokeratinized epithelium and normal underlying connective tissue were detectable (Fig. 5A). The circumvallate papillae showed normal barrel-shaped taste buds (Fig. 6A). Dorsal and ventral surface epithelium revealed a normal thickness, was covered with normal orthokeratin and showed normal underlying connective tissue (Fig. 7A and 8A).

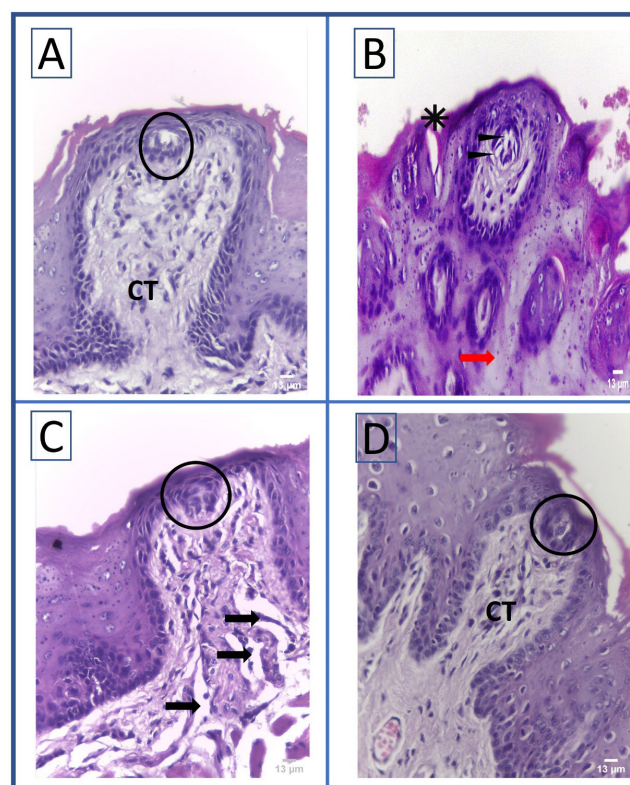


Fig. 4. Photomicrograph of the fungiform papillae

A – group 1 (control) showing normal mushroom-like papillae with well-defined connective tissue (CT) and barrel-shaped taste buds (circle); B – group 2 (STZ) showing disruption in the papillae, a detached keratin layer (asterisk), connective tissue degeneration (red arrow), and taste buds with intracellular vacuolation (black arrow heads); C – group 3 (STZ + BV) showing mushroom-like papilla and barrel-shaped taste buds (circle) besides areas of connective tissue degeneration (black arrows); D – group 4 (STZ + BMSCs) showing mushroom-like papillae with well-defined connective tissue (CT) and normal barrel-shaped taste buds (circle). Original magnification $\times 400$, scale bar: 13 μm .

Group 2 (the STZ group) showed disruption in the normal mushroom-like appearance of the fungiform papillae, and areas of a detached keratin layer and connective tissue degeneration. The fungiform papilla-associated taste buds revealed intracellular vacuolation and evidence of degeneration (Fig. 4B). The filiform papillae displayed atrophied, rounded tips, and a thin layer of keratin with areas of detached keratin. Some epithelial cells revealed hyperchromatic nuclei. The underlying connective tissue displayed evidence

Table 3. Descriptive statistics and comparison of blood glucose levels [mg/dL] between the studied groups (ANOVA and Tukey's post hoc test)

Time point	Group 1	Group 2	Group 3	Group 4	p-value
Week 1	118.05 \pm 14.35 ^B	334.14 \pm 22.19 ^A	325.25 \pm 13.93 ^A	316.5 \pm 54.2 ^A	0.000*
Week 2	114.14 \pm 14.90 ^B	338.14 \pm 21.09 ^A	327.75 \pm 13.97 ^A	322.9 \pm 49.1 ^A	0.000*
Week 3	113.47 \pm 14.26 ^C	355.61 \pm 18.94 ^A	331.10 \pm 14.85 ^{AB}	325.7 \pm 43.2 ^B	0.000*
Week 4	112.81 \pm 14.37 ^C	361.91 \pm 15.85 ^A	334.54 \pm 14.84 ^B	323.8 \pm 39.0 ^B	0.000*

Data presented as mean \pm standard deviation ($M \pm SD$).

Group 1 – control; group 2 – STZ; group 3 – BV-treated diabetic rats; and group 4 – BMSC-treated diabetic rats. * statistically significant; the values with different superscript letters are significantly different.

of degeneration (Fig. 5B). The circumvallate papillae showed multiple degenerated taste buds, while some taste buds presented the loss of their normal barrel-shaped outline (Fig. 6B). Dorsal surface epithelium revealed a reduced thickness and areas of detached keratin. In a few epithelial cells, hyperchromatic nuclei were detectable. There were areas of connective tissue degeneration and dilated blood vessels (Fig. 7B). The epithelium covering the ventral surface of the tongue showed epithelial atrophy, while the connective tissue showed areas of degeneration and dilated blood vessels (Fig. 8B).

Group 3, treated with BV, showed normal fungiform papillae with a mushroom-like appearance and normal barrel-shaped taste buds, with areas of connective tissue vacuolation (Fig. 4C). The examination of the filiform papillae revealed a thread-like shape, and multiple atrophied, rounded tips with areas of detached keratin (Fig. 5C). The circumvallate papillae showed few degenerated taste buds (Fig. 6C). Dorsal and ventral surface epithelium showed increased epithelial and keratin

thickness as compared to Group 2, and areas of connective tissue degeneration (Fig. 7C and 8C).

The examination of group 4, treated with BMSCs, showed mushroom-like fungiform papillae, with normal barrel-shaped taste buds and well-defined connective tissue (Fig. 4D). Thread-like shaped filiform papillae with few areas of detached keratin were detectable (Fig. 5D). Normal circumvallate papillae with normal barrel-shaped taste buds were evident (Fig. 6D). Dorsal and ventral surface epithelium showed an increase in the epithelium and keratin thickness as compared to groups 2 and 3, and areas of connective tissue degeneration (Fig. 7D and 8D).

Morphometric analysis

The highest number of taste buds within the circumvallate papillae was detected in group 1, while the lowest was recorded in group 2, with a statistically significant difference between the groups ($p < 0.05$). Pairwise comparisons revealed a significantly higher number of taste buds in group 4 as compared to groups 2 and 3 ($p < 0.05$). Also, a significantly higher number was recorded in group 3 as compared to group 2 ($p = 0.002$) (Table 4).

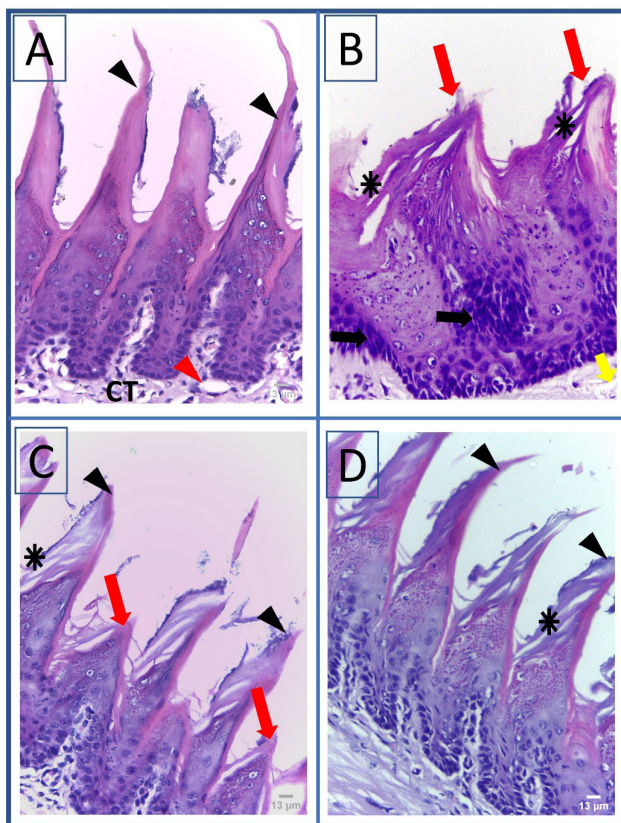


Fig. 5. Photomicrograph of the filiform papillae

A – group 1 (control) showing normal thread-like papillae with orthokeratinized epithelium (black arrow heads), and normal underlying connective tissue (CT) and blood vessels (red arrow head); B – group 2 (STZ) showing the papillae with atrophied rounded tips (red arrows), a detached keratin layer (asterisk), connective tissue degeneration (yellow arrow), and some hyperchromatic nuclei (black arrows); C – group 3 (STZ + BV) showing a thread-like shape (black arrow heads), atrophied, rounded tips (red arrows) and areas of detached keratin (asterisk); D – group 4 (STZ + BMSCs) showing thread-like papillae (black arrow heads) and areas of detached keratin (asterisk). Original magnification $\times 400$, scale bar: 13 μm .

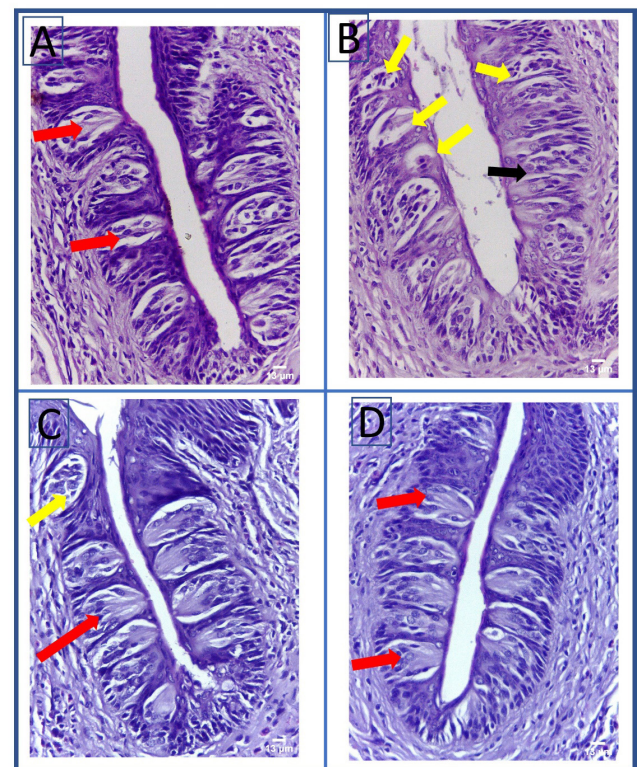


Fig. 6. Photomicrograph of the circumvallate papillae surrounded by a trough with taste buds

A – group 1 (control) showing normal barrel-shaped taste buds (red arrows); B – group 2 (STZ) showing multiple degenerated taste buds (yellow arrows) and taste buds with the loss of their normal barrel-shaped outline (black arrow); C – group 3 (STZ + BV) showing normal barrel-shaped taste buds (red arrows) and few degenerated taste buds (yellow arrow); D – group 4 (STZ + BMSCs) showing normal barrel-shaped taste buds (red arrows). Original magnification $\times 400$, scale bar: 13 μm .

Group 2 was associated with atrophic epithelial changes, with a significantly reduced thickness of both dorsal and ventral surface epithelium as compared to other groups ($p < 0.05$). Groups 3 and 4 effectively increased the epithelial thickness, which showed significantly higher values in both dorsal and ventral surface epithelium as compared to group 2 ($p < 0.05$). Regarding the dorsal and ventral epithelial thickness, a higher mean value was reported for group 4 as compared to group 3. However, the difference was not statistically significant (Table 4).

A reduction in the dorsal epithelial thickness in group 2 as compared to other groups was associated with a significant reduction in the thickness of the basal cell, polyhedral cell, granular cell, and keratin layers ($p < 0.05$) (Table 4).

Both group 3 and group 4 showed a significant increase in the thickness of polyhedral cell, granular cell and keratin layers as compared to group 2 ($p < 0.05$),

whereas the thickness of the basal cell layer showed a significant increase only in group 4 as compared to group 2 ($p < 0.05$). A higher mean value was recorded for the epithelial layer thickness in group 4 as compared to group 3; however, the difference was not statistically significant except for the polyhedral cell layer thickness ($p < 0.05$) (Table 4).

Group 2 showed a significant reduction in the area of the connective tissue papillae ($p < 0.05$). Group 3 had significantly increased connective tissue papillae as compared to groups 2 and 4 ($p < 0.05$). An insignificantly higher mean area of the connective tissue papillae was detected in group 4 as compared to group 2 ($p < 0.05$) (Table 4).

TGF- β 1 and VEGF gene expression

Group 2 showed a significant reduction in *TGF- β 1* and *VEGF* expression as compared to other groups ($p < 0.05$). Group 4 showed a significant increase in *TGF- β 1* and *VEGF* expression as compared to groups 2 and 3 ($p < 0.05$) (Table 5).

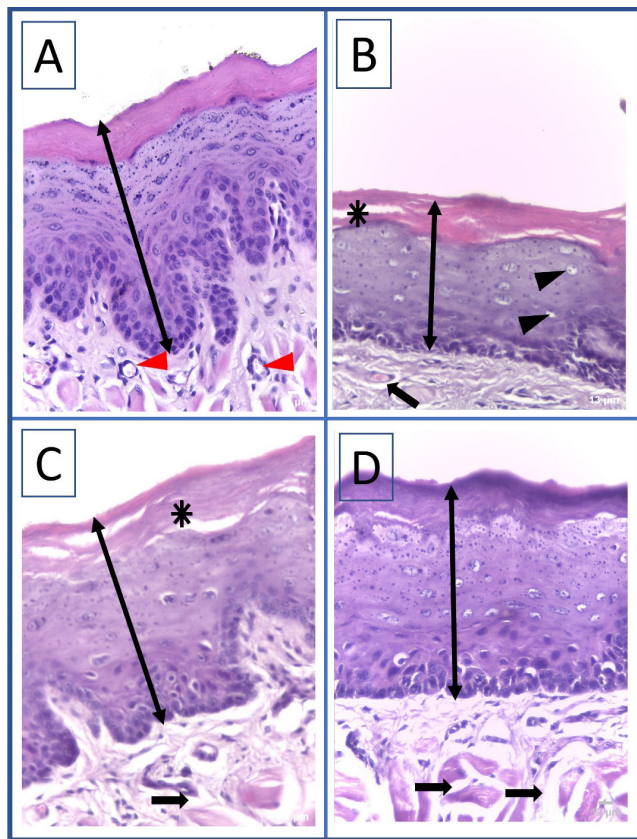


Fig. 7. Photomicrograph of the epithelium covering the dorsal surface of the tongue

A – group 1 (control) showing a normal epithelial thickness (black double arrow), normal orthokeratinized epithelium and normal blood vessels (red arrow heads); B – group 2 (STZ) showing a reduced epithelial thickness (black double arrow), areas of detached keratin (asterisk), intra-epithelial vacuolation (black arrow heads), areas of connective tissue degeneration (black arrow), and dilated blood vessels; C – group 3 (STZ + BV) showing an increased epithelial thickness (black double arrow), areas of detached keratin (asterisk) and areas of connective tissue degeneration (black arrow); D – group 4 (STZ + BMSCs) showing an increase in the epithelium thickness (black double arrow) and areas of connective tissue degeneration (black arrows). Original magnification $\times 400$, scale bar: 13 μ m.

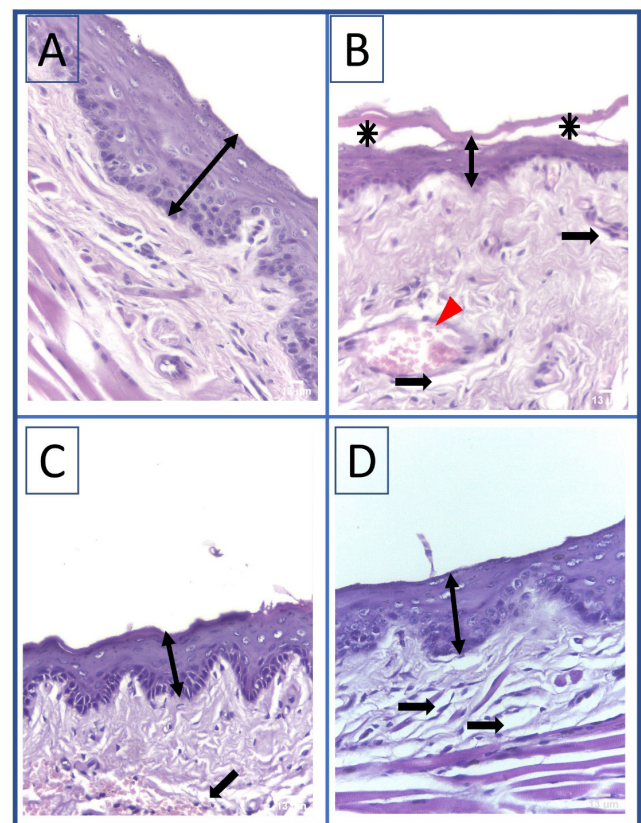


Fig. 8. Photomicrograph of the epithelium covering the ventral surface of the tongue

A – group 1 (control) showing a normal epithelial thickness (black double arrow); B – group 2 (STZ) showing a reduced epithelial thickness (black double arrow), areas of detached keratin (asterisks), areas of connective tissue degeneration (black arrows), and dilated blood vessels (red arrow head); C – group 3 (STZ + BV) showing an increased epithelial thickness (black double arrow) and areas of connective tissue degeneration (black arrow); D – group 4 (STZ + BMSCs) showing an increase in the epithelium thickness (black double arrow) and areas of connective tissue degeneration (black arrows). Original magnification $\times 400$, scale bar: 13 μ m.

Table 4. Morphometric analysis of the studied groups (ANOVA and Tukey's post hoc test)

Parameter	Group	$M \pm SD$	SE	95% CI		F	p-value (ANOVA)
				lower bound	upper bound		
Number of taste buds per circumvallate papilla	group 1 ^A	18.214 \pm 1.323	0.367	17.179	19.249	98.04	0.000*
	group 2 ^D	6.308 \pm 1.601	0.444	5.272	7.343		
	group 3 ^C	9.154 \pm 2.968	0.823	8.118	10.189		
	group 4 ^B	12.183 \pm 0.817	0.227	11.147	13.218		
Dorsal epithelial thickness [mm]	group 1 ^A	237.03 \pm 25.53	7.08	222.53	251.53	28.77	0.000*
	group 2 ^C	145.62 \pm 9.36	2.60	131.12	160.12		
	group 3 ^B	195.44 \pm 7.63	2.11	180.94	209.94		
	group 4 ^{A,B}	212.70 \pm 43.70	12.10	198.20	227.20		
Ventral epithelial thickness [mm]	group 1 ^A	141.64 \pm 27.30	7.57	127.66	155.61	28.10	0.000*
	group 2 ^C	54.65 \pm 5.02	1.39	40.67	68.62		
	group 3 ^B	100.60 \pm 38.50	10.70	86.60	114.50		
	group 4 ^{A,B}	118.41 \pm 16.06	4.45	104.44	132.38		
Basal cell layer thickness [mm]	group 1 ^A	12.725 \pm 1.693	0.470	11.728	13.722	15.89	0.000*
	group 2 ^C	8.265 \pm 2.114	0.586	7.268	9.262		
	group 3 ^{B,C}	9.007 \pm 1.766	0.490	8.010	10.004		
	group 4 ^B	10.621 \pm 1.525	0.423	9.624	11.618		
Polyhedral cell layer thickness [mm]	group 1 ^A	55.87 \pm 14.25	3.95	46.49	65.24	50.19	0.000*
	group 2 ^C	130.28 \pm 12.00	3.33	120.90	139.65		
	group 3 ^B	115.21 \pm 20.51	5.69	105.83	124.50		
	group 4 ^A	84.96 \pm 19.06	5.29	75.58	94.33		
Granular cell layer thickness [mm]	group 1 ^A	62.49 \pm 18.92	5.25	55.65	69.33	17.70	0.000*
	group 2 ^C	29.04 \pm 3.94	1.09	22.21	35.88		
	group 3 ^{B,A}	40.50 \pm 9.67	2.68	33.66	47.34		
	group 4 ^{A,B}	51.01 \pm 11.60	3.22	44.17	57.84		
Keratin layer thickness [mm]	group 1 ^A	44.14 \pm 10.81	3.00	-19.54	0.55	16.41	0.000*
	group 2 ^B	20.82 \pm 1.47	5.29	15.68	25.96		
	group 3 ^A	37.64 \pm 12.55	3.48	-13.43	6.66		
	group 4 ^A	40.76 \pm 6.14	1.70	-7.05	13.05		
Area of the connective tissue papillae [mm ²]	group 1 ^A	2,298.0 \pm 1,648.0	61.8	1,776.9	2,725.4	15.49	0.000*
	group 2 ^B	636.6 \pm 176.2	48.9	162.4	1,110.9		
	group 3 ^A	2,251.2 \pm 222.9	457.0	1,824.0	2,773.0		
	group 4 ^B	698.7 \pm 311.9	86.5	224.5	1,173.0		

SE – standard error; CI – confidence interval; * statistically significant; different superscript letters indicate significant differences between the groups.

Table 5. Descriptive statistics and comparison of *TGF- β 1* and *VEGF* gene expression between the studied groups (ANOVA and Tukey's post hoc test)

Parameter	Group	$M \pm SD$	SE	95% CI		F	p-value (ANOVA)
				lower bound	upper bound		
<i>TGF-β1</i>	group 1 ^A	5.6631 \pm 0.1126	0.0312	5.6092	5.7170	98.04	0.000*
	group 2 ^D	1.0550 \pm 0.0657	0.0182	1.0011	1.1089		
	group 3 ^C	2.2992 \pm 0.0994	0.0276	2.2453	2.3531		
	group 4 ^B	2.8300 \pm 0.1023	0.0284	2.7761	2.8839		
<i>VEGF</i>	group 1 ^A	4.1785 \pm 0.0584	0.0162	4.1386	4.2183	28.77	0.000*
	group 2 ^D	1.0750 \pm 0.0704	0.0195	1.0352	1.1148		
	group 3 ^C	1.6669 \pm 0.0821	0.0228	1.6271	1.7068		
	group 4 ^B	2.0873 \pm 0.0728	0.0202	2.0475	2.1271		

* statistically significant; different superscript letters indicate significant differences between the groups.

Discussion

Diabetes mellitus is a metabolic disorder resulting in multiple complications, including soft tissue abnormalities in the oral cavity. In the present study, we investigated the possible therapeutic effects of BV and BMSCs on the degenerative changes affecting the tongue due to the induction of DM in rats.

Streptozotocin was chosen for DM induction in rats, as it provides a permanent and stable diabetic model. It can induce type I diabetes through the rapid destruction of β -cells in the pancreas.²⁸ In the current study, STZ-induced DM in rats was associated with atrophic changes to the lingual mucosa, with a reduction in the thickness of both dorsal and ventral surface epithelium, the atrophy of the lingual papillae, and a reduction in the number of taste buds per circumvallate papilla. The atrophy of the underlying connective tissue with a significant reduction in the connective tissue papillae was also noticed.

The effect of uncontrolled DM on rats' tongue epithelium and papillae has been previously reported. Streptozotocin-induced DM in rats has been associated with alterations in the distribution and morphology of the fungiform and filiform papillae, with areas of epithelial desquamation,^{29–31} in addition to a significant reduction in the height and width of the filiform papillae.³² Diabetes mellitus has also been associated with the atrophy and a decreased thickness of dorsal surface epithelium,^{32–34} and the atrophy of ventral surface epithelium.³⁴ Lingual epithelial atrophy was observed in rats born to diabetic mothers.³⁵ Epithelial atrophy was also noticeable in the buccal mucosa of diabetic rats.³⁶

In the present study, the circumvallate papillae were impacted by DM. A significant reduction in the number of taste buds per circumvallate papilla has been reported in previous studies.^{27,37} These changes were attributed to a DM-associated reduction in the innervation of taste buds.²⁷ Additionally, rats with induced DM were prone to increased apoptosis of circumvallate papilla taste buds, which was associated with the downregulation of Bcl-2, the upregulation of Bax, and increased activation of caspase-9 and caspase-3.³⁷

Diabetes mellitus has also been linked to the atrophy of the lamina propria underlying the lingual mucosa. A decrease in the height and cross-sectional area of the connective tissue papillae of the dorsal surface of the tongue in rats with induced DM has been previously reported.^{26,31} In addition to the atrophied gingival lamina propria,^{25,38} DM was also linked to an increased incidence of *Candida albicans* and the thickening of bacterial colonies on the dorsal surface of the tongue.²⁹

On the other hand, some reports demonstrated that DM was associated with epithelial hypertrophy.^{25,38} The thickness of the gingival epithelium, and of the prickle cell, granular cell and keratin layers was significantly higher in

rats with induced DM as compared to the control group.²⁵ A statistically significant increase in the thickness of the gingival epithelium, and of the basal, prickle cell, granular, and keratin layers was also observed.³⁸ This indicates that regional variations in the oral tissues can affect the mucosal response to chemically induced DM in rats.

The atrophic effect of DM on the lingual mucosa can be traced back to the diabetes effect on epithelial cells, as DM has been associated with reduced keratinocyte proliferation³⁹ and increased cellular apoptosis.⁴⁰ Reduced cell proliferation, in addition to increased cellular apoptosis, can result in epithelial atrophy. The effect of DM on cellular functions has been attributed to high blood glucose levels, the accumulation of advanced glycation end-products (AGEs), increased tissue hypoxia, and increased levels of reactive oxygen species (ROS) in DM.^{41–43} Diabetes mellitus can also cause systemic inflammation and a chronic inflammatory infiltrate in the oral connective tissues, which can negatively affect the integrity and function of the oral mucosa.^{44–47} Additionally, diabetic microangiopathy may lead to subsequent connective tissue degeneration and mucosal atrophy.^{25,26,48} It has been observed that DM is also linked to an increased expression of p53 in rats³³ and an increased expression of p16.³²

The positive effect of BV on the lingual mucosa observed in the current study reflects its potent biological properties. Bee venom shows anti-inflammatory,⁴⁹ antibacterial⁵⁰ and antioxidant effects.⁵¹ In addition, BV has demonstrated anti-cancerous effects^{52,53} and anti-obesity effects.⁵³ It also has an anti-diabetic effect, as it can lower a blood glucose level, increase the secretion of insulin⁵³ and enhance diabetic wound healing.^{51,53–56} The anti-inflammatory activity of BV could be attributed to melittin, its main constituent, as melittin inhibits the enzymatic activity of phospholipase A2.⁵¹ The phospholipase A2 enzyme is released in severe inflammatory disorders and causes tissue damage.

Bone marrow mesenchymal stem cells effectively improved the morphology of the lingual papillae, increased the number of taste buds per circumvallate papilla and effectively reversed DM-associated epithelial atrophy. Similar to our findings, BMSCs effectively reversed atrophic changes in the fungiform and filiform papillae,^{30,34,57} lingual mucosa,³⁴ and increased the ventral epithelial thickness in rats with STZ-induced DM.³⁴ Bone marrow mesenchymal stem cells were also reported to improve the morphology of both the circumvallate and foliate papillae, and restore their taste buds in rats with STZ-induced DM.⁵⁸ The regenerative effect of BMSC on the lingual mucosa can be attributed to the ability of the cells to release different signaling molecules, including growth factors, cytokines and chemokines, in addition to their anti-inflammatory effect.⁵⁹

The ability of BMSCs to restore the lingual mucosa in diabetic rats can be partly attributed to their angiogenic effect. Bone marrow mesenchymal stem cells can induce

angiogenesis in diabetic wounds through the release of pro-angiogenic factors, including hypoxia-inducible factor (HIF), VEGF, angiopoietin, and erythropoietin,^{60,61} in addition to their ability to differentiate into endothelial cells.⁶¹ They can also secrete multiple growth factors, including epidermal growth factor (EGF), insulin-like growth factor 1 (IGF-1) and platelet-derived growth factor (PDGF), important for the chemotaxis and function of cells responsible for diabetic wound healing.^{62,63} The cells also have immunomodulatory properties. They can interact with cells of the innate and adaptive immune systems to downregulate pro-inflammatory cytokines, including interleukin 1 beta (IL-1 β), tumor necrosis factor alpha (TNF- α) and IL-6, and to upregulate anti-inflammatory cytokines – IL-10 and prostaglandin E2 (PGE2).⁶⁴ Bone marrow mesenchymal stem cells can also increase the migration, proliferation and function of keratinocytes in diabetic wounds, and induce re-epithelialization.^{63,65} Taken together, the ability of BMSCs to stimulate angiogenesis and keratinization, and their immunomodulatory properties can explain their potential to reverse the diabetes-associated atrophic changes observed in the lingual mucosa of rats in the current study.

In this study, the levels of TGF- β 1 and VEGF were investigated to define their role in enhancing the regeneration of the tongue following BV and BMSC treatment in diabetic rats. Treatment with BV and BMSCs resulted in the upregulation of both TGF- β 1 and VEGF in comparison with the levels observed in the diabetic rats in group 2.

The molecular mechanisms underlying the regeneration of damaged tongue tissues following BV treatment in group 3 may be related to the ability of BV to upregulate TGF- β 1, which stimulates the migration of keratinocytes and increases integrin expression.⁶⁶ Transforming growth factor beta 1 can induce collagen expression.⁶⁷ Also, BV enhances the expression of VEGF, which in turn stimulates local angiogenesis through mobilizing and recruiting bone marrow-derived endothelial progenitor cells, thereby decreasing impaired healing in diabetic rats.⁵¹

According to Kwon et al., the regenerative potential of BMSCs in tongue tissues in diabetic rats appeared to provide better results when compared to the untreated animals, which was explained by the local upregulation of cytokines and growth factors.⁶² Bone marrow mesenchymal stem cells increase the expression of TGF- β 1 moderately and of VEGF markedly, which in turn enhances the inflammatory response, and induces the recruitment and proliferation of cells, required for repairing damaged tissues. Additionally, the immunoblotting analysis revealed an increased expression of neovascularization-related genes, such as TGF- β 1 and VEGF, in a BMSC-treated mouse burn injury model.⁶⁸ In the present study, group 2 (diabetic rats) displayed the lowest VEGF levels, which might be due to the inability of diabetic rats to properly upregulate VEGF expression in response to hypoxia.²⁰

Conclusions

Diabetes mellitus exerted detrimental effects on rat tongues. Therapy with BV and BMSCs ameliorated the damaging effects of DM by upregulating the expression of TGF- β 1 and VEGF. However, BMSC therapy promoted better results in regenerating the diseased tissues.

Ethics approval and consent to participate

This study was approved by the Institutional Animal Care and Use Committee (IACUC) at Cairo University, Egypt (approval No. CU III F 74 18). This research was conducted in compliance with the ARRIVE (Animal Research: Reporting of In Vivo Experiments) guidelines and regulations (<https://arriveguidelines.org>). The maintenance and care of the experimental animals conformed with the International Guiding Principles for Biomedical Research Involving Animals.

Data availability


The datasets generated and/or analyzed during the current study are available from the corresponding author on reasonable request.


Consent for publication


Not applicable.

ORCID iDs

Israa Ahmed Radwan  <https://orcid.org/0000-0001-8262-5941>

Dina Rady  <https://orcid.org/0000-0002-9672-6935>

Mohamed Ramadan  <https://orcid.org/0000-0002-5090-2243>

Sara El Moshy  <https://orcid.org/0000-0002-2860-8523>

References

- Sandu MM, Protasiewicz DC, Firănescu AG, Lăcătușu EC, Bicu ML, Moța M. Data regarding the prevalence and incidence of diabetes mellitus and prediabetes. *Rom J Diabetes Nutr Metab Dis*. 2016;23(1):95–103. <http://www.rjdnmd.org/index.php/RJDNMD/article/view/111>. Accessed January 10, 2022.
- Park J, Jang HJ. Anti-diabetic effects of natural products an overview of therapeutic strategies. *Mol Cell Toxicol*. 2017;13(1):1–20. doi:10.1007/s13273-017-0001-1
- Standards of medical care in diabetes – 2017: Summary of revisions. *Diabetes Care*. 2017;40(Suppl 1):S4–S5. doi:10.2337/dc17-S003
- Hossen MS, Gan SH, Khalil MI. Melittin, a potential natural toxin of crude bee venom: Probable future arsenal in the treatment of diabetes mellitus. *J Chem*. 2017;2017:4035626. doi:10.1155/2017/4035626
- Raghuraman H, Chattopadhyay A. Melittin: A membrane-active peptide with diverse functions. *Biosci Rep*. 2007;27(4–5):189–223. doi:10.1007/s10540-006-9030-z
- Abdela N, Jilo K. Bee venom and its therapeutic values: A review. *Adv Life Sci Tech*. 2016;44:18–22. <https://www.iiste.org/Journals/index.php/ALST/article/view/30404>. Accessed March 10, 2022.
- Sforzin JM, Bankova V, Kuropatnicki AK. Medical benefits of honey-bee products. *Evid Based Complement Alternat Med*. 2017;2017:2702106. doi:10.1155/2017/2702106
- Morgan NG, Montague W. Stimulation of insulin secretion from isolated rat islets of Langerhans by melittin. *Biosci Rep*. 1984;4(8):665–671. doi:10.1007/BF01121020

9. Granero-Moltó F, Weis JA, Miga MI, et al. Regenerative effects of transplanted mesenchymal stem cells in fracture healing. *Stem Cells*. 2009;27(8):1887–1898. doi:10.1002/stem.103
10. Si YL, Zhao YL, Hao HJ, Fu XB, Han WD. MSCs: Biological characteristics, clinical applications and their outstanding concerns. *Ageing Res Rev*. 2011;10(1):93–103. doi:10.1016/j.arr.2010.08.005
11. Bernardi S, Severini GM, Zauli G, Secchiero P. Cell-based therapies for diabetic complications. *Exp Diabetes Res*. 2012;2012:872504. doi:10.1155/2012/872504
12. Ezquer M, Arango Rodriguez M, Giraud-Billoud MG, Ezquer F. Mesenchymal stem cell therapy in type 1 diabetes mellitus and its main complications: From experimental findings to clinical practice. *J Stem Cell Res Ther*. 2014;4(8):1000227. doi:10.4172/2157-7633.1000227
13. Dang LTT, Phan NK, Truong KD. Mesenchymal stem cells for diabetes mellitus treatment: New advances. *Biomed Res Ther*. 2017;4(1):1062–1081. doi:10.15419/bmrar.v4i1.144
14. Spanheimer RG, Umpierrez GE, Stumpf V. Decreased collagen production in diabetic rats. *Diabetes*. 1988;37(4):371–376. doi:10.2337/diab.37.4.371
15. Papadimitriou A, Peixoto EB, Silva KC, Lopes de Faria JM, Lopes de Faria JB. Inactivation of AMPK mediates high phosphate-induced extracellular matrix accumulation via NOX4/TGF β -1 signaling in human mesangial cells. *Cell Physiol Biochem*. 2014;34(4):1260–1272. doi:10.1159/000366336
16. Al-Mulla F, Leibovich SJ, Francis IM, Bitar MS. Impaired TGF- β signaling and a defect in resolution of inflammation contribute to delayed wound healing in a female rat model of type 2 diabetes. *Mol Biosyst*. 2011;7(11):3006–3020. doi:10.1039/c0mb00317d
17. Gerber HP, Hillan KJ, et al. VEGF is required for growth and survival in neonatal mice. *Development*. 1999;126(6):1149–1159. doi:10.1242/dev.126.6.1149
18. Bogdanov S. Bee venom: Composition, health, medicine: A review. 2015;1:1–20.
19. Alhadlaq A, Mao JJ. Mesenchymal stem cells: Isolation and therapeutics. *Stem Cells Dev*. 2004;13(4):436–448. doi:10.1089/scd.2004.13.436
20. Lerman OZ, Galiano RD, Armour M, Levine JP, Gurtner GC. Cellular dysfunction in the diabetic fibroblast: Impairment in migration, vascular endothelial growth factor production, and response to hypoxia. *Am J Pathol*. 2003;162(1):303–312. doi:10.1016/S0002-9440(10)63821-7
21. Lima PH, Sinzato YK, Gelaleti RB, Calderon IM, Rudge MV, Damasceno DC. Genotoxicity evaluation in severe or mild diabetic pregnancy in laboratory animals. *Exp Clin Endocrinol Diabetes*. 2012;120(5):303–307. doi:10.1055/s-0031-1299766
22. Mousavi SM, Imani S, Haghighi S, Mousavi SE, Karimi A. Effect of Iranian honey bee (*Apis mellifera*) venom on blood glucose and insulin in diabetic rats. *J Arthropod Borne Dis*. 2012;6(2):136–143. PMID:23378971. PMCID:PMC3547303.
23. Abdel Aziz MT, El Asmar MF, Atta HM, et al. Efficacy of mesenchymal stem cells in suppression of hepatocarcinogenesis in rats: Possible role of Wnt signaling. *J Exp Clin Cancer Res*. 2011;30(1):49. doi:10.1186/1756-9966-30-49
24. Schneider CA, Rasband WS, Eliceiri KW. NIH Image to ImageJ: 25 years of image analysis. *Nat Methods*. 2012;9(7):671–675. doi:10.1038/nmeth.2089
25. Yasuda K, Uemura M, Suwa F. Morphological study of the palatal gingiva of the maxillary first molar in the type 2 diabetes mellitus model rat. *Okajimas Folia Anat Jpn*. 2011;88(2):65–74. doi:10.2535/ofaj.88.65
26. Uemura M, Tamada Y, Suwa F. Morphological study of the connective tissue papillae and the capillary loops on the lingual dorsum in the type 2 diabetes mellitus model rats. *Okajimas Folia Anat Jpn*. 2009;85(4):139–149. doi:10.2535/ofaj.85.139
27. Pai MH, Ko TL, Chou HC. Effects of streptozotocin-induced diabetes on taste buds in rat vallate papillae. *Acta Histochem*. 2007;109(3):200–207. doi:10.1016/j.acthis.2006.10.006
28. Lenzen S. The mechanisms of alloxan- and streptozotocin-induced diabetes. *Diabetologia*. 2008;51(2):216–226. doi:10.1007/s00125-007-0886-7
29. Ortug F, Ignak S, Ortug A. Characteristics of lingual papillae in diabetic rats. *Morphologie*. 2018;102(339):250–254. doi:10.1016/j.morpho.2018.08.003
30. Mohamed Mohsen RO, Halawa AM, Hassan R. Role of bone marrow-derived stem cells versus insulin on filiform and fungiform papillae of diabetic albino rats (light, fluorescent and scanning electron microscopic study). *Acta Histochem*. 2019;121(7):812–822. doi:10.1016/j.acthis.2019.07.007
31. Eltokhey HM. The influence of ozonized olive oil gel on the dorsal surface of the tongue of streptozotocin induced diabetic albino rats. *J Am Sci*. 2013;9(10):193–201. https://www.jofamericanscience.org/journals/am-sci/am0910/025_20597am0910_193_201.pdf. Accessed January 10, 2022.
32. Altun E, Yazici H, Arslan E, Tulaci KG, Erken HA. The impact of type II diabetes on tongue dysplasia and p16-related aging process: An experimental study. *Anal Cell Pathol (Amst)*. 2019;2019:3563215. doi:10.1155/2019/3563215
33. Abd-Elmotelb MA. Morphometric, histological and immunohistochemical study of tongue epithelium in diabetic rats. *Life Sci J*. 2018;15:1–6. doi:10.7537/marslsj151118.01
34. Fakhri M, Hegazy E, Ghali LS. Effect of stem cells versus statins on the mucous membrane and salivary glands of the tongue of induced-diabetic rats. *Suez Canal Univ Med J*. 2017;20(2):190–200. doi:10.21608/SCUMJ.2017.136419
35. El-Beeh ME, Fouda YA, El-badry DA, El-Sayyad HI. Antiapoptotic activity of cinnamon on some organs of 18 days rat fetuses of diabetic mother. *Biosci Biotech Res Asia*. 2019;16(3):637–648. doi:10.13005/bbra/2779
36. Caldeira EJ, Garcia PJ, Minatel E, Camilli JA, Alves Cagnon VH. Morphometric analysis and ultrastructure of the epithelium of the oral mucosa in diabetic autoimmune NOD mice. *Braz J Morphol Sci*. 2017;21(4):197–205. <http://www.jms.periodikos.com.br/article/587cb4557f8c9d0d058b45f9/pdf/jms-21-4-587cb4557f8c9d0d-058b45f9.pdf>. Accessed January 10, 2022.
37. Cheng B, Pan S, Liu X, Zhang S, Sun X. Cell apoptosis of taste buds in circumvallate papillae in diabetic rats. *Exp Clin Endocrinol Diabetes*. 2011;119(8):480–483. doi:10.1055/s-0031-1279714
38. Dağ A, Fırat ET, Uysal E, Ketani MA, Şeker U. Morphological changes caused by streptozotocin-induced diabetes in the healthy gingiva of rats. *Exp Clin Endocrinol Diabetes*. 2016;124(03):167–172. doi:10.1055/s-0035-1559781
39. Zhang C, Ponugoti B, Tian C, et al. FOXO1 differentially regulates both normal and diabetic wound healing. *J Cell Biol*. 2015;209(2):289–303. doi:10.1083/jcb.201409032
40. Graves DT, Liu R, Alikhani M, Al-Mashat H, Trackman PC. Diabetes-enhanced inflammation and apoptosis – impact on periodontal pathology. *J Dent Res*. 2006;85(1):15–21. doi:10.1177/154405910608500103
41. Brizeno LA, Assreuy AM, Alves AP, et al. Delayed healing of oral mucosa in a diabetic rat model: Implication of TNF- α , IL-1 β and FGF-2. *Life Sci*. 2016;155:36–47. doi:10.1016/j.lfs.2016.04.033
42. Lan CCE, Liu IH, Fang AH, Wen CH, Wu CS. Hyperglycaemic conditions decrease cultured keratinocyte mobility: Implications for impaired wound healing in patients with diabetes. *Br J Dermatol*. 2008;159(5):1103–1115. doi:10.1111/j.1365-2133.2008.08789.x
43. Sada K, Nishikawa T, Kukidome D, et al. Hyperglycemia induces cellular hypoxia through production of mitochondrial ROS followed by suppression of aquaporin-1. *PLoS One*. 2016;11(7):e0158619. doi:10.1371/journal.pone.0158619
44. Batbayar B, Zelles T, Vér A, Fehér E. Plasticity of the different neuropeptide-containing nerve fibres in the tongue of the diabetic rat. *J Peripher Nerv Syst*. 2004;9(4):215–223. doi:10.1111/j.1085-9489.2004.09402.x
45. Awwad RA, Abd Rabbo RA. Comparative histological study on the effect of *Allium sativum* (garlic), *Allium cepa* (onion) and insulin on lingual papillae of diabetic rats. *Egypt J Histo*. 2020;43(2):598–613. doi:10.21608/EJH.2020.26939.1267
46. Dağ A, Fırat ET, Uysal E, Ketani Ş, Ketani MA. Histological investigation of the impact of streptozotocin-induced experimental diabetes on the healthy gingivae of rats. *Biotechnol Biotechnol Equip*. 2014;28(4):710–715. doi:10.1080/13102818.2014.943558
47. Pahwa R, Goyal A, Jialal I. *Chronic Inflammation*. In: StatPearls [Internet]. Treasure Island, FL: StatPearls Publishing; 2023. <https://www.ncbi.nlm.nih.gov/books/NBK493173>. Accessed March 10, 2022.

48. Akai K, Uemura M, Suwa F. Morphological study of the palatine mucosa in the type 2 diabetes mellitus model rat. *J Osaka Dent Univ.* 2013;47(2):185–194. https://www.osaka-dent.ac.jp/faculty/dent_grad/gakui/apache/otu_1577_txt.pdf. Accessed April 15, 2022.
49. Jeong CH, Cheng WN, Bae H, et al. Bee venom decreases LPS-induced inflammatory responses in bovine mammary epithelial cells. *J Microbiol Biotechnol.* 2017;27(10):1827–1836. doi:10.4014/jmb.1706.06003
50. Otręba M, Marek Ł, Tyczyńska N, Stojko J, Rzepecka-Stojko A. Bee venom, honey, and royal jelly in the treatment of bacterial infections of the oral cavity: A review. *Life (Basel).* 2021;11(12):1311. doi:10.3390/life11121311
51. Badr G, Hozzein WN, Badr BM, Al Ghamdi A, Saad Eldien HM, Garraud O. Bee venom accelerates wound healing in diabetic mice by suppressing activating transcription factor-3 (ATF-3) and inducible nitric oxide synthase (iNOS)-mediated oxidative stress and recruiting bone marrow-derived endothelial progenitor cells. *J Cell Physiol.* 2016;231(10):2159–2171. doi:10.1002/jcp.25328
52. Amar S, Mustafa El-Bolok AH, El-Gayar SF, Sholkamy MI. Synergistic cytotoxic effect of honey bee venom and cisplatin on tongue squamous cell carcinoma cell line. *Open Access Maced J Med Sci.* 2021;9(8):1739–1744. doi:10.3889/oamjms.2021.7672
53. Bogdanov S. Chapter 1: Biological and therapeutic properties of bee venom. In: *The Bee Venom Book*. Mühlethurnen, Switzerland: Bee Product Science; 2015.
54. Al-Waili N, Hozzein WN, Badr G, et al. Propolis and bee venom in diabetic wounds; a potential approach that warrants clinical investigation. *Afr J Tradit Complement Altern Med.* 2015;12(6). doi:10.4314/ajtcam.v12i6.1
55. Kurek-Górecka A, Komosinska-Vassev K, Rzepecka-Stojko A, Olczyk P. Bee venom in wound healing. *Molecules.* 2020;26(1):148. doi:10.3390/molecules26010148
56. Hozzein WN, Badr G, Badr BM, et al. Bee venom improves diabetic wound healing by protecting functional macrophages from apoptosis and enhancing Nrf2, Ang-1 and Tie-2 signaling. *Mol Immunol.* 2018;103:322–335. doi:10.1016/j.molimm.2018.10.016
57. El-Sherif N, Abou El Ftooh MM, Mubarak R, Rady D. Regenerative potential of platelet rich plasma and bone marrow derived mesenchymal stem cells on the lingual mucosa in streptozotocin-induced diabetic rats. *Ann Romanian Soc Cell Biol.* 2021;25(6):16334–16347. <https://annalsofrscb.ro/index.php/journal/article/view/8882>. Accessed April 15, 2022.
58. Mohamed Mohsen RO, Halawa AM, Hassan R. Comparative study between the effectiveness of bone marrow derived stem cells and insulin on circumvallate and foliate papillae of diabetic rats: Histological and morphological study. *Ain Shams J Dent Sci.* 2020;1(1):1–14. doi:10.21608/ASJDS.2019.12043.1003
59. Fui LW, Lok MPW, Govindasamy V, Yong TK, Lek TK, Das AK. Understanding the multifaceted mechanisms of diabetic wound healing and therapeutic application of stem cells conditioned medium in the healing process. *J Tissue Eng Regen Med.* 2019;13(12):2218–2233. doi:10.1002/term.2966
60. Wei L, Fraser JL, Lu ZY, Hu X, Yu SP. Transplantation of hypoxia preconditioned bone marrow mesenchymal stem cells enhances angiogenesis and neurogenesis after cerebral ischemia in rats. *Neurobiol Dis.* 2012;46(3):635–645. doi:10.1016/j.nbd.2012.03.002
61. King A, Balaji S, Keswani SG, Crombleholme TM. The role of stem cells in wound angiogenesis. *Adv Wound Care (New Rochelle).* 2014;3(10):614–625. doi:10.1089/wound.2013.0497
62. Kwon DS, Gao X, Liu YB, et al. Treatment with bone marrow-derived stromal cells accelerates wound healing in diabetic rats. *Int Wound J.* 2008;5(3):453–463. doi:10.1111/j.1742-481X.2007.00408.x
63. Kato J, Kamiya H, Himeno T, et al. Mesenchymal stem cells ameliorate impaired wound healing through enhancing keratinocyte functions in diabetic foot ulcerations on the plantar skin of rats. *J Diabetes Complications.* 2014;28(5):588–595. doi:10.1016/j.jdiacomp.2014.05.003
64. Moreira A, Kahlenberg S, Hornsby P. Therapeutic potential of mesenchymal stem cells for diabetes. *J Mol Endocrinol.* 2017;59(3):R109–R120. doi:10.1530/JME-17-0117
65. Cao Y, Gang X, Sun C, Wang G. Mesenchymal stem cells improve healing of diabetic foot ulcer. *J Diabetes Res.* 2017;2017:9328347. doi:10.1155/2017/9328347
66. Vaday GG, Schor H, Rahat MA, Lahat N, Lider O. Transforming growth factor- β suppresses tumor necrosis factor α -induced matrix metalloproteinase-9 expression in monocytes. *J Leukoc Biol.* 2001;69(4):613–621. doi:10.1189/jlb.69.4.613
67. Zhao D, Shi Y, Dang Y, Zhai Y, Ye X. Daidzein stimulates collagen synthesis by activating the TGF- β /smad signal pathway. *Australas J Dermatol.* 2015;56(1):e7–e14. doi:10.1111/ajd.12126
68. Oh EJ, Lee HW, Kalimuthu S, et al. In vivo migration of mesenchymal stem cells to burn injury sites and their therapeutic effects in a living mouse model. *J Control Release.* 2018;279:79–88. doi:10.1016/j.jconrel.2018.04.020